Received: 19 April 2023 | Revised: 30 July 2023 | Accepted: 31 July 2023

DOI: 10.1111/jnc.15936

Journal of Neurochemistry JNC The Official Journal of the International Society for Neurochemistry WILEY

ORIGINAL ARTICLE

Functional effects of haemoglobin can be rescued by haptoglobin in an in vitro model of subarachnoid haemorrhage

Hannah Warming[1,2] | Katrin Deinhardt[1] | Patrick Garland[3] | John More[3] | Diederik Bulters[4] | Ian Galea[5] | Mariana Vargas-Caballero[1]

[1]School of Biological Sciences, Faculty of Environmental and Life Sciences, University of Southampton, Southampton, UK

[2]Department of Physiology, Anatomy and Genetics, University of Oxford, Oxford, UK

[3]Bio Products Laboratory Limited, Elstree, UK

[4]Department of Neurosurgery, Wessex Neurological Centre, University Hospital Southampton NHS Foundation Trust, Southampton, UK

[5]Clinical Neurosciences, Clinical and Experimental Sciences, Faculty of Medicine, University of Southampton, UK

Correspondence
Mariana Vargas-Caballero, School of Biological Sciences, Faculty of Environmental and Life Sciences, University of Southampton, Southampton SO17 1BJ, UK.
Email: m.vargas-caballero@soton.ac.uk

Ian Galea, Clinical Neurosciences, Clinical and Experimental Sciences, Faculty of Medicine, University of Southampton SO16 6YD, UK.
Email: i.galea@soton.ac.uk

Diederik Bulters, Department of Neurosurgery, Wessex Neurological Centre, University Hospital Southampton NHS Foundation Trust, Southampton SO16 6YD, UK.
Email: dbulters@nhs.net

Funding information
Gerald Kerkut Charitable Trust; Institute for Life Sciences, University of Southampton

Abstract

During subarachnoid haemorrhage, a blood clot forms in the subarachnoid space releasing extracellular haemoglobin (Hb), which causes oxidative damage and cell death in surrounding tissues. High rates of disability and cognitive decline in SAH survivors are attributed to loss of neurons and functional connections during secondary brain injury. Haptoglobin sequesters Hb for clearance, but this scavenging system is overwhelmed after a haemorrhage. Whilst exogenous haptoglobin application can attenuate cytotoxicity of Hb in vitro and in vivo, the functional effects of sub-lethal Hb concentrations on surviving neurons and whether cellular function can be protected with haptoglobin treatment remain unclear. Here we use cultured neurons to investigate neuronal health and function across a range of Hb concentrations to establish the thresholds for cellular damage and investigate synaptic function. Hb impairs ATP concentrations and cytoskeletal structure. At clinically relevant but sub-lethal Hb concentrations, we find that synaptic AMPAR-driven currents are reduced, accompanied by a reduction in GluA1 subunit expression. Haptoglobin co-application can prevent these deficits by scavenging free Hb to reduce it to sub-threshold concentrations and does not need to be present at stoichiometric amounts to achieve efficacy. Haptoglobin itself does not impair measures of neuronal health and function at any concentration tested. Our data highlight a role for Hb in modifying synaptic function in surviving neurons, which may link to impaired cognition or plasticity after SAH and support the development of haptoglobin as a therapy for subarachnoid haemorrhage.

Abbreviations: AMPA, α-amino-3-hydroxy-5-methyl-4-isoxazoleproprionic acid; ATP, adenosine triphosphate; CSF, cerebrospinal fluid; DIV, day in vitro; EPSC, excitatory post-synaptic current; EPSP, excitatory post-synaptic potential; Hb, haemoglobin; Hp, haptoglobin; mEPSC, miniature excitatory post-synaptic current; RBC, red blood cell; SAH, subarachnoid haemorrhage; SBI, secondary brain injury.

Diederik Bulters, Ian Galea and Mariana Vargas-Caballero are joint senior authors.

KEYWORDS
excitability, haptoglobin, patch clamp, subarachnoid haemorrhage, synaptic transmission

1 | INTRODUCTION

Subarachnoid haemorrhage (SAH) causes irreversible damage to brain tissues both during the acute phase and in secondary brain injury (SBI), leading to a high fatality rate of 30–40% (Hackett & Anderson, 2000; Petridis et al., 2017) and significant disability in many survivors (English, 2020; Luoma & Reddy, 2013). Raised intracranial pressure, oedema, inflammation and vasospasm lead to acute and delayed ischaemic damage and have limited treatment options (Diringer, 2009; Diringer et al., 2011; Luoma & Reddy, 2013; Van Gijn & Rinkel, 2001). Following a haemorrhage red blood cells (RBCs) begin to lyse, leading to the accumulation of cell-free haemoglobin (Hb) in the cerebrospinal fluid (CSF). The Hb tetramer degrades into Hb dimers, hemichromes and eventually haem and free iron. Iron-containing products permeate into tissues, exposing neurons and other cells to oxidative stress (Yeh & Alayash, 2003). Hb breakdown products such as met-Hb and haem can also cause inflammation, exacerbating damage and further contributing to SBI (Belcher et al., 2014; Kwon et al., 2015). Hb and iron toxicity significantly contribute towards development of vasospasm and SBI (Akeret et al., 2021; Hugelshofer et al., 2019; Joerk et al., 2014), but are not currently clinically targeted.

Cell-free Hb leads to neuronal cell death in vitro (Jungner et al., 2020; Regan & Panter, 1993; Wang et al., 2002) and in vivo (Garton et al., 2016; Zille et al., 2017) with key mediators being oxidative stress and ferroptosis caused by redox-active haem and iron, released from Hb (Bai et al., 2020; Li et al., 2017). More recently, research has suggested functional changes to neurons after exposure to Hb, such as reductions in synaptic anchoring proteins, neuroligins and neurexins (Shen et al., 2015) leading to reduced formation of excitatory synapses. The pre-synaptic marker synaptophysin and post-synaptic protein PSD-95 were down-regulated in a mouse model of prolonged Hb exposure in ventricular and subarachnoid spaces (Garland et al., 2020). In two rat blood injection models of SAH these biochemical changes were accompanied by cognitive deficits, indicating neurotransmission may be altered (Sasaki et al., 2016). Further evidence shows that long-term potentiation (LTP), the synapse-strengthening process thought to underlie learning and memory (Bliss & Collingridge, 1993), was impaired in a rat pre-chiasmatic injection model of SAH (Tariq et al., 2010). Hb-mediated impairments in synaptic plasticity as suggested by rodent studies may help explain poor rates of recovery seen in SAH, in addition to cognitive changes that affect quality of life in survivors (Al-Khindi et al., 2010; Tidswell et al., 1995). Despite strong evidence linking Hb accumulation and iron deposition in the brain to neurodegeneration, both in SAH and a number of other neurodegenerative diseases (Jellinger, 1999; Núñez et al. 2012; Patel et al. 2002), functional data on neuronal activity in the presence of Hb is limited.

Free Hb measured in the CSF after SAH is highly variable and peaks at around 10 μM (Akeret et al., 2021; Garland et al., 2020) between day 10–12 after the haemorrhage thus presenting a wide therapeutic window for clinical intervention targeting Hb neurotoxicity. Haptoglobin (Hp) functions as an effective Hb scavenger by binding irreversibly to Hb and preventing haem release. Hp is present in blood plasma within the range of 0.3–3 mg/mL (Galea et al., 2012; Kazmi et al., 2019; Thomsen et al., 2013). However, the large multimeric Hp proteins do not easily cross the blood–brain barrier, hence the concentration of Hp is much lower in the central nervous system compared to the systemic circulation (Galea et al., 2012), and Hp is rapidly depleted in the cerebrospinal fluid (CSF) after SAH (Akeret et al., 2021). Enhancing the CSF concentration of Hp in vivo can protect against cell loss, synaptic marker alteration, associated behavioural deficits (Garland et al., 2020) and vasospasm (Garland et al., 2020; Hugelshofer et al., 2019). Furthermore, Hp administration has been used in clinical trials to prevent Hb-mediated kidney damage in sickle-cell anaemia and blood transfusion without significant adverse effects (Gando & Tedo, 1994; Schaer et al., 2013), indicating good peripheral tolerance.

Here we build on this knowledge by investigating the functional effects of persistent Hb exposure in neurons, measuring neuronal health and synaptic activity to understand the effects of clinically relevant Hb concentrations in the brain and how this may impact secondary brain injury after SAH. CSF analyses show that neurons experience extended exposure to 10 μM or more free Hb after SAH (Akeret et al., 2021; Garland et al., 2020) and the composition of Hb species changes within the first days and weeks after SAH because of the conversion of Hb to met-Hb and dissociation into haem and free iron. This can be observed in vivo based on the paramagnetic properties of oxy-Hb, deoxy-Hb and met-Hb using magnetic resonance imaging (MRI), such that the composition of the blood clot appears distinctly different at SAH onset and in the days and weeks that follow (Janick et al., 1991; Siddiqui et al., 2011). Research has shown a delay in the onset of Hb-mediated cell death in neuronal culture, with cell loss starting 8 h after application (Regan & Panter, 1993) suggesting that breakdown of Hb is likely implicated in its pathogenic effects. Whilst the exact timeline of Hb catabolism is uncertain in the brain environment, we chose to measure function of cells in vitro after 48 h and 1 week of Hb application, based on key changes to Hb composition assessed by neuroimaging.

We also studied the potential of Hp to prevent Hb-induced deficits, whilst considering the practical difficulties of the therapeutic agent reaching the haematoma and interstitial free Hb in a clinical setting. For example, it is not likely to fully perfuse all CSF spaces with Hp after SAH, as a result of the density of the haematoma interfering with CSF flow (Zhou et al., 2022). High variability of free Hb concentration seen in patients after SAH will also be affected by the bleed volume, location and other factors (Akeret et al., 2021),

so accurately predicting Hb content and scavenging all free Hb is difficult. Additionally, not all free Hb is able to be bound by Hp in vivo: whilst the majority of Hb can be scavenged, there is a fraction of Hb that undergoes structural changes related to degradation or oxidative stress (Garland et al., 2020) and cannot be bound by Hp. Hb permeates the outer cortex, as evidenced by an inward diminishing gradient of iron deposition after SAH (Galea et al., 2022), and it may be difficult for a therapeutic agent delivered in the CSF space to permeate the cortex in areas with closely apposed blood clot. Finally, the CSF is a purposely low-protein fluid (Galea, 2021) and high CSF protein content is associated with poor outcome after SAH (Nadkarni et al., 2020), which limits the amount of protein that can be administered intrathecally. For these reasons, we investigated a partial, rather than stoichiometric, scavenging of free Hb by Hp, to understand the threshold of free Hb that is tolerated by neurons. This will improve understanding of the effects of Hb on neuronal function and add to the body of knowledge needed to develop Hp as a clinical therapeutic in SAH.

2 | MATERIALS AND METHODS

2.1 | Haemolysate preparation

Human blood was obtained from human volunteers after informed consent (National Research Ethics Service approval 11/SC/0204). Blood was collected in heparin tubes (BD, UK) and transferred to a centrifuge tube onto a layer of histopaque-1077 (Sigma-Aldrich, 30% of final volume). The tube was centrifuged at 900G for 15 min and red blood cells (RBCs) in the lower fraction were isolated. RBCs were washed with sterile Dulbecco's PBS until supernatant was clear and colourless, before lysing with distilled water. Following centrifugation at 20000 *g* for 30 min to remove ghost membranes, supernatant was removed, filtered (15 μm) and the protein concentration was determined (Pierce™) before storage at −80°C. The haemoglobin species composition assessed by spectrophotometry was comprised on average of 79.8 ± 1.4% oxyhaemoglobin, 13.2 ± 1.3% deoxyhaemoglobin and 7.0 ± 2.0% methaemoglobin (Benesch et al., 1973). These relative proportions are similar to those seen in a primate SAH model in vivo (Pluta et al., 1998). Haemolysate (HL) concentration is expressed as a concentration of dimers, hence 10 μM HL is equivalent to 20 μM of iron-containing haem.

2.2 | Source of haptoglobin and scavenging analyses

Hp was prepared by Bio Products Laboratory Ltd from pooled human blood plasma, enriched for Hp1 dimer. Hp was dialysed with a molecular cut off of 14 kDa and endotoxin content was measured at <0.02 E.U./ml. Hp molar concentration refers to a weighted average molecular weight of monomers, in the purified mixture of Hp1 and Hp2.

To determine rate of free Hb scavenging, a fixed amount of HL was incubated with increasing amounts of Hp overnight at room temperature and 2 μg of Hb from each mix separated on a non-denaturing 8% polyacrylamide gel. Hb band density was analysed against a HL-only control lane per gel to quantify the percentage of unbound Hb at each ratio. A binding curve from three gel repeats was used to estimate the concentration of free Hb in treatment groups with co-application of Hp throughout experiments.

2.3 | Animal husbandry and primary neuron culture

Animal care and experimental procedures were conducted in accordance with U.K. Home Office regulations under the Animals (Scientific Procedures) Act of 1986 working under Schedule 1 and approved by the University of Southampton Ethics (ERGO 65253). C57/BL6 mice (Charles River) were bred in-house under a 12/12 hr light/dark cycle at 21°C in individually ventilated cages with ad libitum access to water and food. Mice were bred in pairs or trios, and dam weight was approximately 40 g. Neonatal mice (P0) of undetermined sex and weight were culled by cervical dislocation followed by confirmation of permanent cessation of circulation. We selected cervical dislocation as a Schedule 1 method instead of the alternative method of anaesthetic overdose as it can be performed rapidly and avoids the discomfort associated with needle puncture in addition to distress prior to anaesthetic action.

P0 mice were chosen to avoid usage of excess animals (littermates and dam) in the alternative method of embryonic cultures.

Two to four animals from each litter were used per culture and dissected in Dulbecco's PBS without calcium or magnesium (Gibco), and hippocampi isolated, pooled and dissociated with papain before seeding onto poly-D-lysine coated glass coverslips at 1000 cells/mm^2. Cells were incubated with Neurobasal Medium supplemented with 1% Glutamax-I and 2% B27 (Gibco), incubated at 37°C with 5% CO_2. A full media change was carried out at DIV7 and HL and/or Hp applied after randomised allocation to culture wells alongside a media volume top-up at DIV14. Treatment groups were blinded until raw data analysis was complete for each experiment. A total of 135 neonatal mice were used for neuronal cultures across all groups, with some cultures used only for electrophysiology and others used in additional experiments such as microscopy.

2.4 | ATP assay

Primary cultures were washed once with supplemented Neurobasal Medium and then fresh medium applied, and the CellTitre Glo assay kit (Promega) carried out at room temperature to measure adenosine triphosphate (ATP) levels. The kit was used as per manufacturer instructions. Background luminescence was measured and subtracted from readings using media, and results were unblinded and normalised to vehicle-treated cells within cultures.

2.5 | Immunofluorescent staining and microscopy

Neuron cultures were fixed at DIV21 with 4% paraformaldehyde, permeabilised with 0.1% Triton X-100 and washed in tris-buffered saline. Cells were blocked using goat serum and stained with anti-tubulin 1:400 (Cell Signalling 2128) followed by Alexa Fluor secondary antibodies at 1:1000 in 2% goat serum. Coverslips were mounted with Fluoroshield ab104139, Abcam containing DAPI and imaged using an Olympus IX83 inverted microscope with a 40X air objective. Images were acquired using Cellsens software and processed by background subtraction using a radius of 50 pixels and overlaid using FIJI software (Schindelin et al., 2012). Treatment groups were blinded from the point of treatment application until image processing was completed, and fields of view were chosen using DAPI channel.

2.6 | Patch clamp electrophysiology

Cells were analysed at DIV21 ± 1. Signals were low-pass filtered at 5 kHz using an Axopatch 200B amplifier and acquired at 20 kHz using a National Instruments board analogue to digital converter. MATLAB software (Mathworks), custom software (Ginj2.0, Hugh P.C. Robinson) and WinEDR software (Strathclyde) were used for data acquisition. Borosilicate glass micropipettes were pulled to a resistance of 5–7 MΩ and filled with solution containing, in mM, 125 potassium gluconate, 10 KCl, 10 HEPES, 10 Phosphocreatine, 0.4 GTP, 4 Mg-ATP and pH balanced to 7.3 using KOH. These pipettes had an initial break-in series resistance of typically 16 MΩ. Whole-cell recordings were discarded if the initial series resistance exceeded the maximum upper value of 30 MΩ or if the initial series resistance changed by more than 20%. Extracellular artificial CSF contained, in mM, 126 sodium chloride, 2 $CaCl_2$, 10 glucose, 2 $MgSO_4$, 3 KCl and 26.4 sodium carbonate. The liquid junction potential of −12.5 mV was not corrected for. Artificial CSF was bubbled with 95% O_2, 5% CO_2 throughout and maintained at 25 ± 1°C.

Passive membrane properties were measured using voltage-clamp, and cells excluded if the input resistance exceeded 1 GΩ indicating non-pyramidal cells (Schilling & Eder, 2015). The first 3 recorded cells to meet these criteria in each culture were included for analysis. Active membrane properties were measured using a current-step injection stimulus in bridge-compensated current clamp, and current injection to maintain cells at −70 mV. Evoked EPSPs were recorded from connected pairs of cells. A positive current injection of 500–1000 pA with duration 6 msec was applied to induce a single action potential and measure a post-synaptic response repeated at 0.14 Hz. Evoked EPSCs were recorded from post-synaptic cells in the same manner, in bridge mode. Paired-pulse ratio was measured from EPSCs with a 50 ms interval. Miniature EPSCs (mEPSCs) were recorded at −70 mV using a Cs-gluconate based intracellular solution containing, in mM, gluconic acid 70, CsCl 10, NaCl 5, BAPTA 10, HEPES 10, QX-314 10, GTP-NaCl 0.3, ATP-Mg 4 and adjusted to pH 7.3 using 1 M CsOH. ACSF contained 500 nM tetrodotoxin and 1 μM SR-95531. The liquid junction potential for Cs-gluconate solution of −12 mV was not corrected for.

2.7 | Polyacrylamide gel electrophoresis

Protein lysates were collected at DIV21 for Western blotting and separated in 7% SDS polyacrylamide gels using electrophoresis. Proteins were transferred to nitrocellulose membranes and stained using anti-GluA1 antibody (13 185, Cell Signalling) secondary antibody & imaged using an infrared scanner (Odyssey®, LI-COR Biosciences). Blot quantification was carried out using ImageStudio software (LI-COR). For Hb-Hp binding experiments, a fixed amount of Hb was incubated with varying Hp at room temperature overnight and the resulting mixtures separated using non-denaturing 8% polyacrylamide gel electrophoresis before staining with Coomassie, loading 2 μg of Hb per lane. Gels were de-stained in 10% methanol with 7% glacial acetic acid overnight, imaged and quantified against a control lane containing 2 μg of unbound Hb within each gel.

2.8 | Excitatory post-synaptic potential analysis

mEPSC recordings were analysed with Eventer software (Winchester et al., 2020) with a low-pass filter of 1000 Hz. A machine-learning model was trained using approximately 2500 mEPSC events from each treatment group, detected using Pearson method with a threshold of 4 standard deviations of the noise. Training took place by manually accepting or rejecting events based on appropriate rise and decay kinetics. The model was then employed to detect events in each mEPSC recording and report inter-event interval and peak amplitude for the first 500 events per cell. Intrinsic membrane properties and evoked EPSP and EPSC amplitude were analysed from raw data using custom-written MATLAB code. Evoked currents and potentials were averaged from 50 to 100 repeats per cell, 3 cells per independent culture with automatic event onset detection. Statistical analyses were performed in GraphPad Prism V9 (GraphPad Software) using a two-way repeated measures ANOVA with matching within cultures and Dunnett's post-hoc corrections. We did not assume data sphericity in experiments where data were normalised within each culture, and epsilon ($\hat{\epsilon}$) is reported when the Geisser–Greenhouse correction has been applied in these analyses. Data are represented as mean ± SEM. For all analyses, results were considered significant if $p < 0.05$.

2.9 | Sample size

No sample size was calculated a priori. For our variables with no significant difference, we performed Monte Carlo simulations in MATLAB using our data sets to test if a difference would be observed in measures of membrane potential, input resistance or rheobase as

well as mEPSC frequency. In each case, we concluded that our n was sufficient to detect physiologically meaningful effect sizes if present. For example we would be able to detect a 5 mV effect size with 98% power (mean −72 mV, SEM 2.5 mV, sample size $n=9$ cultures, 10000 iterations in Monte Carlo simulation), although to be able to detect a change in 1 mV in resting membrane potential would have considerably less power of 12%.

3 | RESULTS

3.1 | Haemolysate disrupts ATP levels and neurite structure in vitro

To characterise the threshold for neuronal damage by Hb in our neuronal culture system we applied HL prepared from human RBCs to hippocampal neuronal cultures at DIV14 and measured ATP concentration in the lysed cell population using the luciferase-based CellTitre Glo assay. HL application started at 10 μM of Hb dimer as measured in human CSF after SAH (Garland et al., 2020) and was applied up to 200 μM. We observed a dose-dependent reduction in ATP starting at 50 μM HL at 48 h ($F(2.4, 23.6)=520.8$, $\hat{\varepsilon}=0.48$, $p<0.0001$, Figure 1a) and from 20 μM after 1 week of HL application ($F(2.5, 29.9)=713.6$, $\hat{\varepsilon}=0.5$, $p<0.0001$, Figure 1b). To assess neurite structure, we imaged neurons using immunofluorescent staining of β-tubulin and DAPI. At all concentrations of HL, neurite beading indicative of microtubule disruption was observed after a 1-week incubation, which worsened with increasing concentration of HL (Figure 1c).

3.2 | Haemolysate neurotoxicity can be prevented with haptoglobin

To determine if Hp can prevent HL-induced toxicity, we co-applied Hp with HL to cells for 1 week and repeated ATP measurements. Hp alone at 30 μM appeared to show an increase in ATP ($F(2.58, 25.8)=40.4$, $\hat{\varepsilon}=0.51$, $p<0.0001$, Figure 2a) but all other concentrations up to 120 μM were not different to vehicle conditions indicating that Hp does not reduce ATP levels in neuronal cell cultures even at very high concentrations.

Next, we investigated whether partial scavenging could protect from neurotoxicity by binding one-third of free Hb with co-applied Hp. We measured ATP levels after co-applying Hp with HL for 1 week and found that scavenging 34 ± 3.6% of free Hb, reducing free Hb from 20 to 13.2 ± 0.7 μM, was sufficient to prevent an ATP deficit ($F(1.2, 9.7)=12.4$, $\hat{\varepsilon}=0.61$, $p=0.004$, Figure 2b). We further investigated 50 μM HL with increasing Hp concentrations and found that the ATP deficit was not prevented by scavenging one-third of free Hb, but could only be prevented when the majority of free Hb was bound by Hp ($F(2.2, 43.8)=124.9$, $\hat{\varepsilon}=0.44$, $p<0.0001$, Figure 2c). These data suggest that Hp can prevent ATP deficits in neuron cultures at high concentrations of Hb, by scavenging free Hb to sublethal levels. The threshold for a Hb-induced ATP deficit appeared to lie between 13.2–20 μM free Hb. Staining of β-tubulin in the same neuronal cultures after incubation with 50 μM HL and co-application of Hp showed neurite beading in all conditions with free Hb, and microtubules were restored to vehicle morphology under conditions of full Hb scavenging (Figure 2d).

3.3 | Sub-lethal haemolysate does not alter intrinsic membrane properties of neurons

Previous data had shown that free Hb perturbs the resting membrane potential (RMP) of neurons (Yip et al., 1996) and these effects may be driven by changes in neuronal excitability or ongoing synaptic activity. To investigate the functional effects of HL on the excitability of neuronal cultures we measured intrinsic membrane properties of neurons at DIV21 ± 1 in whole-cell patch clamp electrophysiology, after a 1-week exposure to HL or Hp in culture medium. 10 μM Hb, which has been measured as the average peak in human CSF after SAH (Garland et al., 2020) does not appear to cause an ATP deficit and was, therefore, used as a clinically relevant yet sub-lethal HL insult for electrophysiological studies. As such we could use visualised patch clamp to record from neurons randomly selected from a large population. Since scavenging one-third of free Hb restored ATP deficits using 20 μM HL, we employed the same scavenging ratio when co-applying Hp to 10 μM HL for electrophysiology, reducing the free Hb concentration in culture medium from 10 μM to approximately 6.4 ± 0.4 μM.

We found no effect of treatment on the RMP of neurons ($F(3, 54)=0.2451$, $p=0.86$) or input resistance ($F(3, 54)=1.34$, $p=0.27$ (Figure 3a,b). We applied a current injection stimulus to the cells and analysed the rheobase ($F(3, 54)=1.08$, $p=0.36$, Figure 3c,d). Finally, we quantified the number and frequency of action potentials fired at each current injection step (Figure 3e,f), and there was no effect of treatment (action potential number: $F(3, 15)=0.52$, $p=0.68$, maximum frequency: $F(3, 15)=0.85$, $p=0.49$). The same membrane properties were also measured at 48 h of exposure to HL or Hp, with no effect of treatment across all analyses (data are not shown).

Our data indicate that cultured neurons can maintain their intrinsic membrane properties throughout a one-week exposure to 10 μM HL. This corroborates the finding that there is no disturbance to ATP levels in these cultures at this concentration.

3.4 | 10 μM HL reduces AMPA receptor-mediated synaptic currents

We investigated synaptic function in neurons exposed to HL by measuring mEPSCs. These currents represent the activation of α-amino-3-hydroxy-5-methyl-4-isoxazolepropionic acid (AMPA) receptors because of spontaneous fusion of pre-synaptic vesicles and glutamate release. There was no change in frequency of mEPSCs (treatment effect $F(3, 54)=1.98$, $p=0.13$, Figure 4ai,b), but we observed a reduction in amplitude in the presence of HL compared to vehicle ($F(3, 54)=4.99$, $p=0.004$, HL vs vehicle

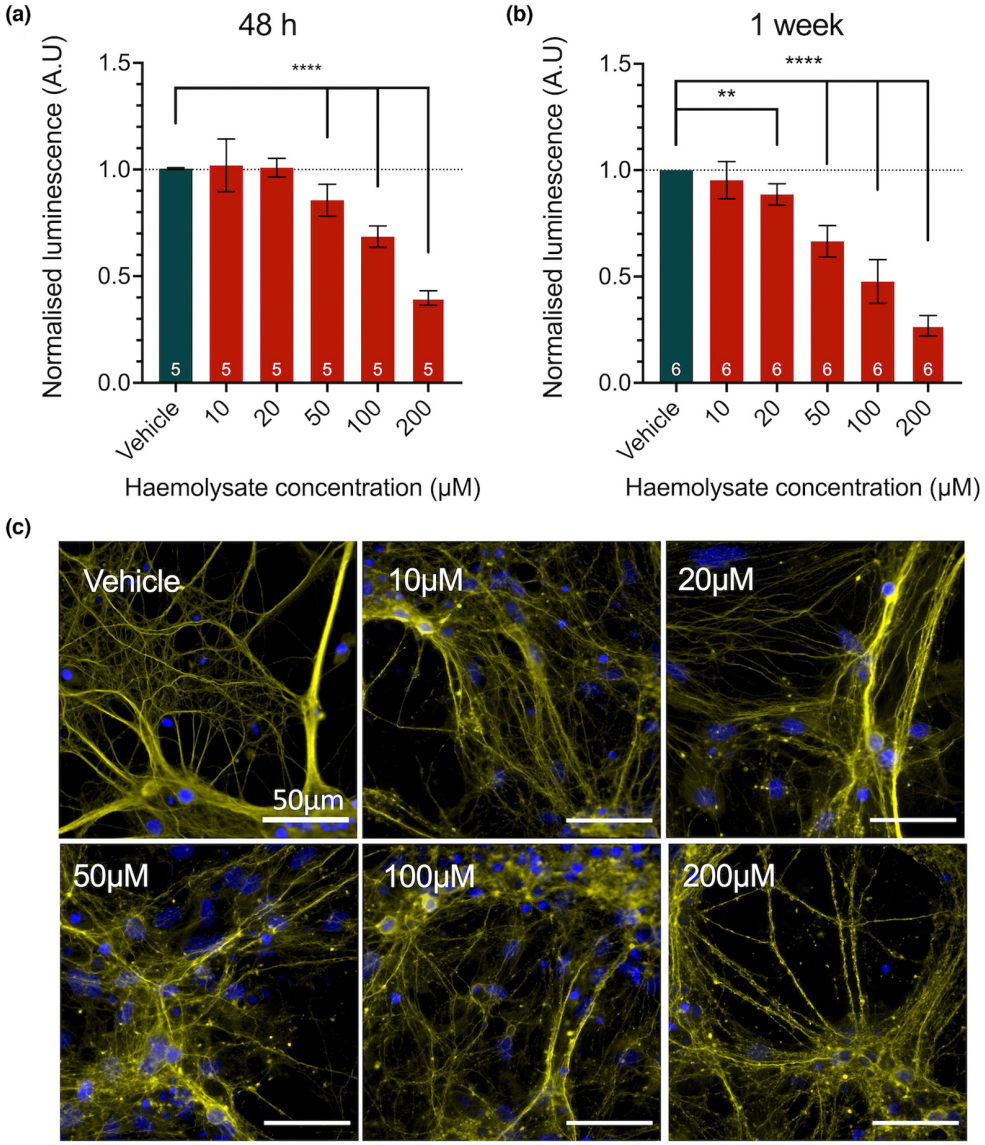

FIGURE 1 Haemolysate impairs ATP levels and neurites in cultured neurons. (a) The CellTitre Glo assay found a reduction in ATP concentration after 48 h and (b) 1 week of exposure to haemolysate. (c) β-tubulin staining shows disruption of microtubules by haemolysate after 1 week. $^{**}p<0.01$, $^{****}p<0.0001$.

$p=0.001$, Figure 4aii–c), which was not observed with Hp co-application ($p=0.18$).

Next, we quantified unitary EPSPs in connected cell pairs. After a 1-week exposure to 10 μM HL, EPSP amplitude was significantly decreased ($F(3, 24)=3.54$, $p=0.03$, HL vs vehicle $p=0.01$, Figure 5a,b) and this was prevented when Hp was co-applied to reduce free Hb (vehicle vs HL + Hp: $p=0.15$). We also quantified the unitary EPSC, which showed a similar reduction in amplitude in the presence of HL ($F(3, 24)=3.41$, $p=0.034$, HL vs vehicle $p=0.015$) but not when Hp was also present ($p=0.16$, Figure 5c,d). The paired-pulse ratio was not different across conditions ($F(3, 24)=0.48$, $p=0.70$, Figure 5c,e), nor was the failure rate (vehicle: 3.39 ± 2.2%, HL 3.5 ± 2.7%; treatment effect $F(3, 24)=1.57$, $p=0.22$).

When HL and Hp were co-applied, AMPAR currents were not significantly different to HL alone, but were not different from vehicle conditions either. This indicates Hp was providing a partial rescue of synaptic AMPAR currents. To ensure Hp was not suppressing AMPAR-mediated currents, we measured evoked EPSP and EPSC amplitude at a higher concentration of 24 μM Hp and found no difference to vehicle (EPSP amplitude: vehicle 1.93 ± 0.34 mV, Hp 24 μM 2.47 ± 0.59 mV, $p=0.48$. EPSC current: vehicle 42.6 ± 11.7 pA, Hp 24 μM 41.3 ± 15.2 pA, $p=0.95$. $N=3$ pairs).

3.5 | 10 μM haemolysate reduces GluA1 expression

To assess if the protein levels of one of the major subunit components of AMPA receptors, GluA1, is affected by HL exposure we prepared protein lysates from cell cultures at DIV21 after 1 week of

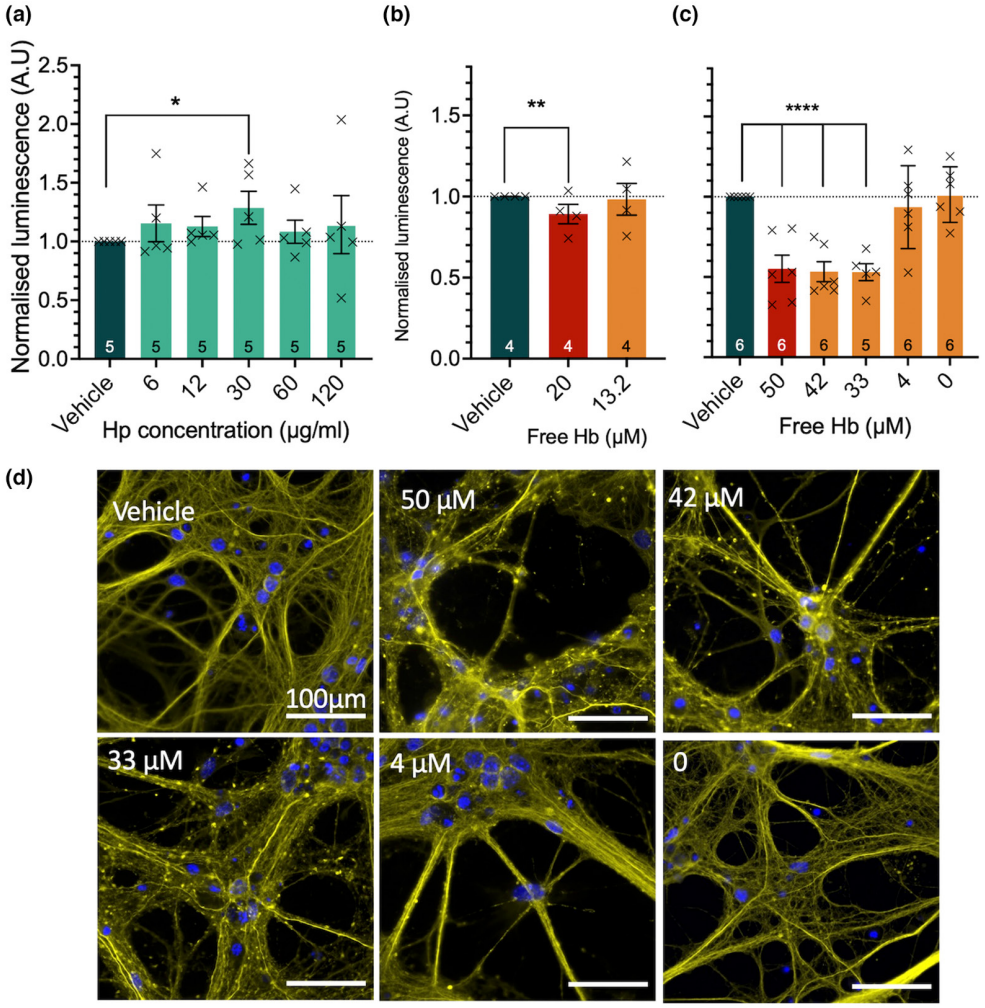

FIGURE 2 Haptoglobin can prevent deficits in ATP and neurite structure caused by haemolysate. (a) ATP levels in cultured neurons after 1 week of exposure to haptoglobin (b) ATP levels after incubation with 20 µM of HL (red bars) and co-application of Hp to scavenge one-third of free Hb (orange). (c) 50 µM HL co-applied with increasing amounts of Hp to scavenge free Hb. (d) β-tubulin staining shows disrupted microtubule morphology after incubation with 50 µM HL and co-application of Hp, expressed as concentration of free Hb remaining in media. $^{*}p<0.05$, $^{**}p<0.01$, $^{****}p<0.0001$.

incubation with 10 µM HL with or without Hp and separated using SDS-PAGE and Western blotting. Membranes were probed for GluA1 and normalised to β-tubulin (Figure 6a). We found a reduction in GluA1 expression in cells exposed to HL ($F(3, 12)=5.12$, $p<0.05$, HL Vs Vehicle $p<0.05$) but not when Hp was co-applied ($p=0.20$, Figure 6b) indicating down-regulation of GluA1 protein in the presence of unbound Hb.

4 | DISCUSSION

We investigated the effects of Hb at concentrations relevant for SAH on neuronal health and synaptic activity and determined whether partiall scavenging of free Hb can prevent functional deficits in neurons. SAH features a complex variety of pathological mechanisms contributing to acute damage and secondary brain injury, which have been extensively reviewed (Budohoski et al., 2014; Neifert et al., 2021; Righy et al., 2015). Hb accumulation in the subarachnoid space through haemolysis exposes neurons to an average of 10 µM Hb in CSF and possibly higher concentrations at the site of the haematoma between 10 and 12 days after SAH onset, as seen in human CSF analyses (Akeret et al., 2021; Garland et al., 2020). CSF Hb concentrations have been proposed as a diagnostic marker for SBI, with a proposed threshold of 7.1 µM of tetrameric Hb (Akeret et al., 2021) equivalent to 14.2 µM of Hb dimer, similar to our data. In another study, the average Hb peak concentration in CSF was higher in patients who developed delayed ischaemic neurological deficits (10 µM) than those who did not (6 µM) (Hugelshofer et al., 2018). This evidence suggests that the level of CSF Hb is directly linked to SBI and, therefore, poor recovery after SAH and scavenging Hb to reduce its concentration in the brain has potential as a therapeutic intervention.

To first characterise the threshold of free Hb that causes damage within our neuronal culture model, we measured ATP levels in the

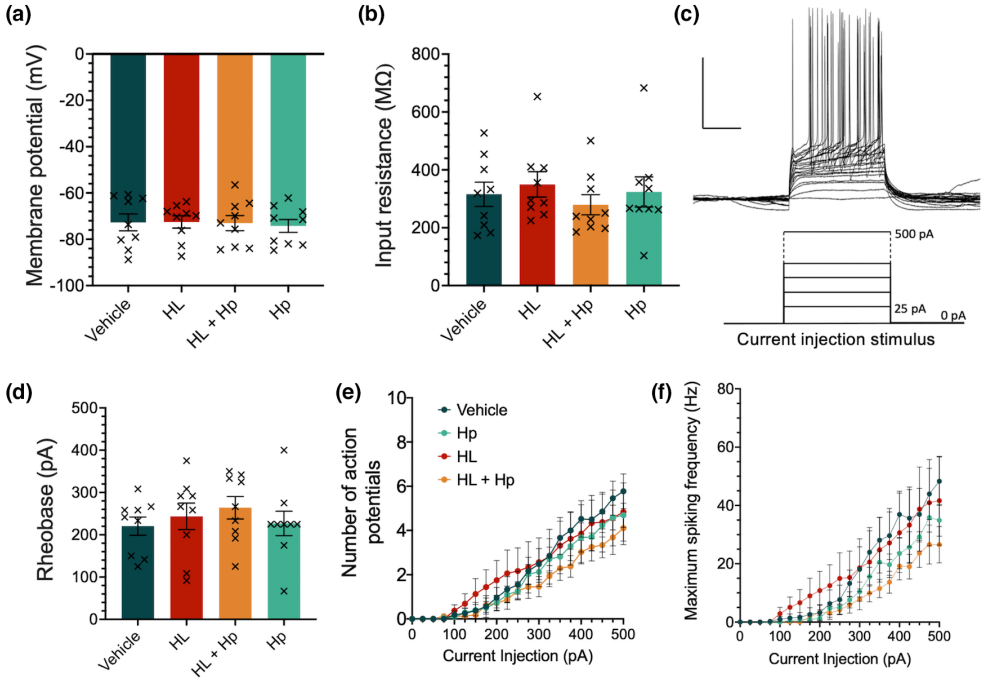

FIGURE 3 Intrinsic neuronal membrane properties are not altered by 10 μM Hb within 1 week. (a) Membrane potential and (b) input resistance are measured upon break-in to the cell in whole-cell patch clamp. (c) A current injection stimulus in steps of 25 pA is applied to the cell in bridge-compensated current clamp. (d) Rheobase measured from a 250 ms current injection in (c). (e) maximum number of action potentials fired and (f) the maximum spiking frequency observed at each current injection step. $N = 3–5$ cells per culture, 9 cultures.

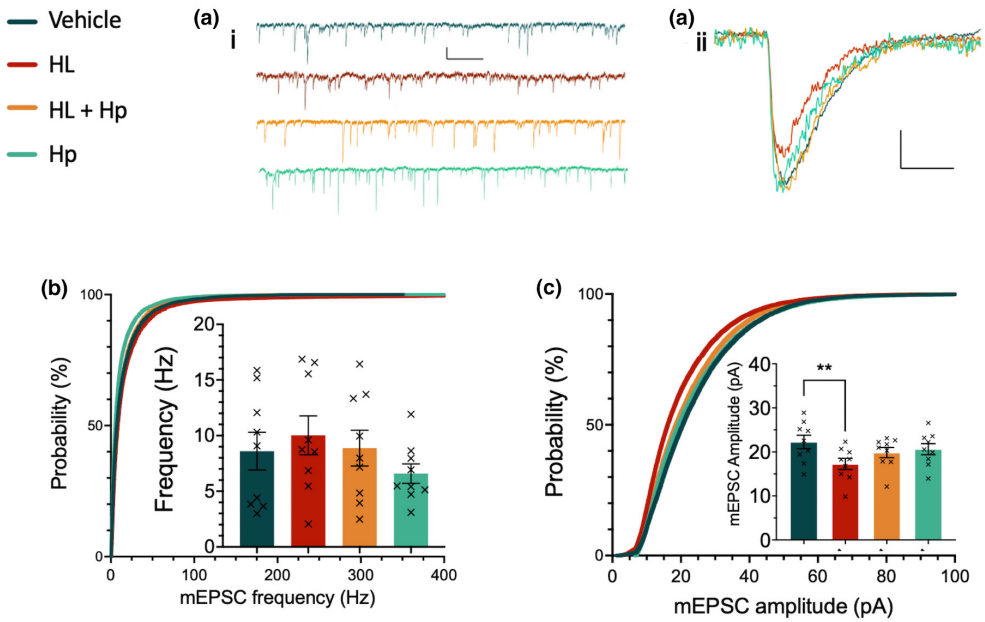

FIGURE 4 Miniature excitatory post-synaptic current (mEPSC) amplitude is reduced by a 1-week exposure to 10 μM HL. (a) Sample traces showing (i) mEPSCs (scale bar 1 s/10 pA) and (ii) overlaid individual events (scale bar 10 ms/ 10 pA). (b) Quantification of mEPSC frequency and (c) amplitude as cumulative frequency distribution and median value per culture. $N = 3$ cells per culture, 9 cultures. Significance levels: $^{**}p < 0.01$.

presence of Hb. We found that the threshold for an ATP deficit at 48 h (50 μM) was higher than that at 1 week (20 μM), suggesting Hb neurotoxicity occurs progressively as previously suggested (Wang et al. 2002) and impairs ATP levels. This may occur through suppression of metabolic processes or cell death. Primary neuron cultures contain glial cells unless treated with cell cycle inhibitors (Hilgenberg & Smith, 2007; Hui et al., 2016), which provide trophic support and may contribute to ATP levels in these assays. However, evidence suggests that neurons are more vulnerable to Hb-mediated cell loss than glia, as in co-culture models glial cells and oligodendrocytes

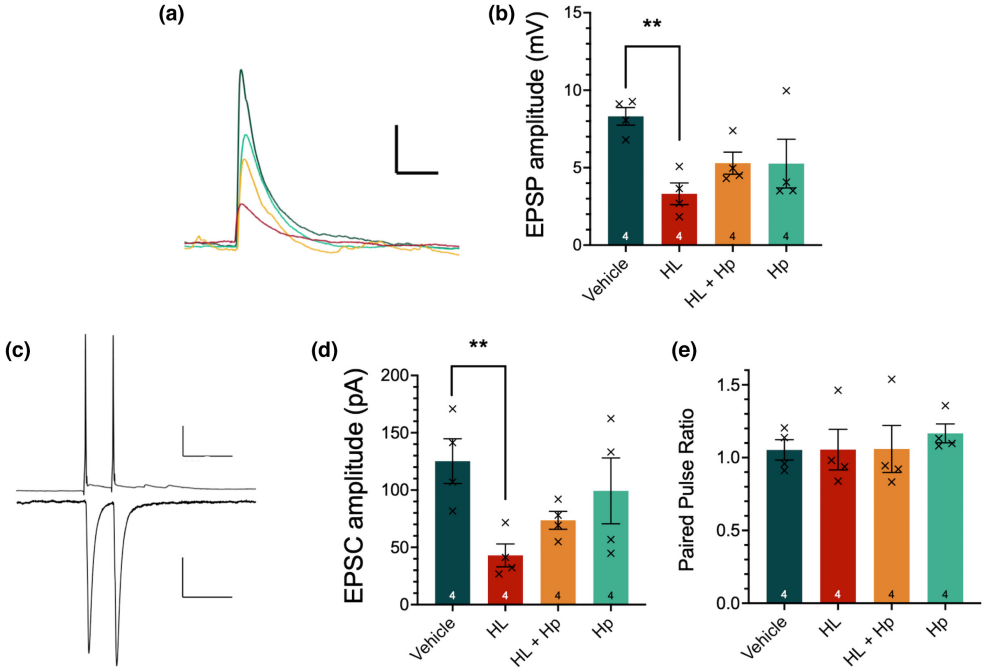

FIGURE 5 Amplitude of evoked excitatory post-synaptic potentials (EPSPs) and excitatory post-synaptic currents (EPSCs) is reduced by 10 μM HL. (a) Representative mean EPSPs (scale bar 50 s/2 mV). (b) Quantification of evoked EPSP amplitude. (c) Paired-pulse sample trace with inter-pulse interval of 50 ms (scale bar top: 100 ms/25 mV, bottom: 100 ms/25 pA). (d) Unitary EPSC amplitude and (e) Paired-pulse ratio. $N = 3$ pairs per culture, 4 cultures. Significance level: $^{**}p < 0.01$.

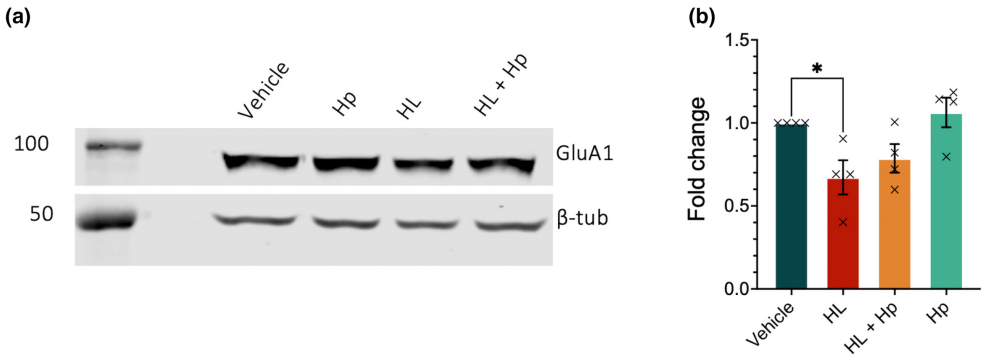

FIGURE 6 Total AMPA receptor GluR1 subunit levels are reduced in hippocampal cell cultures by a 1-week incubation with HL. (a) Hippocampal cell culture lysates were prepared at DIV21 after a 1-week incubation with 10 μM HL or Hp and blots probed for GluR1 and β-tubulin. (b) Quantification of GluA1 normalised to loading control. $N = 3$ cultures. Significance level: $^{*}p < 0.05$.

appear unaffected by Hb exposure at similar concentrations (Jungner et al., 2020; Regan & Guo, 1998; Regan & Panter, 1993). We cannot exclude effects of HL on glia, or of glial cell contribution to ATP levels and, therefore, to identify neuron-specific effects of Hb we immunostained cultured cells for β-tubulin to identify neurites. We observed neurite beading, indicative of cytoskeletal breakdown such as that seen in Wallerian degeneration (Garland et al., 2012) that worsened with increasing concentration of Hb. This occurred even at 10 μM free Hb, where an ATP deficit was not observed, suggesting that microtubule degradation may occur prior to loss of cells or metabolic deficit. Along the same lines, degeneration of axons is seen after SAH in humans as reflected by elevations in CSF neurofilament-light concentration, long considered a key marker of neurodegeneration and this correlated with preceding CSF Hb concentration (Garland et al., 2020, 2021).

We could not assess the relative contribution of oxy-Hb, deoxy-Hb or met-Hb to the neurotoxicity observed in culture. Whilst one does not expect a change in ratio of oxy-Hb to deoxy-Hb with time, a slight gradual rise in met-Hb is possible over a 7 day period in culture, as observed in a primate SAH model (Pluta et al., 1998) and in humans (Akeret et al., 2021). Nevertheless, the Hp binding kinetics of met-Hb are similar to Hb (Gu et al. 2022).

We next investigated the potential of human Hp to protect from Hb-mediated damage, by co-incubating cell cultures with HL

and Hp. The differential efficacy of Hp genotypes in scavenging Hb from the brain and outcome after SAH has been reviewed previously (Gaastra et al., 2017; Sadrzadeh & Bozorgmehr, 2004) with a general consensus that the presence of Hp1 is beneficial, with Hp1-1 and Hp1-2 genotypes having better neuroprotective qualities than Hp2-2. In this study we have used Hp from pooled human blood plasma, containing both isoforms but enriched for Hp1 protein, containing approximately 60% Hp1-1 dimer.

We considered the logistics of Hp infusion into the subarachnoid space containing a peak CSF concentration of 10 μM Hb. Under these conditions, to bind all free Hb based on an average molecular weight for Hp monomers of 52.18 kDa within the Hp preparation used in this study, a CSF Hp concentration of 0.522 g/L would need to be achieved. Protein levels in the CSF in healthy individuals vary in the range 0.3–0.4 g/L (Kwon & Kim, 2014; McCudden et al., 2017), increasing to 0.7–0.8 g/L after SAH (Jeffcote & Ho, 2010). High CSF protein is associated with poor outcome after SAH, linked to higher rates of SBI (Nadkarni et al., 2020). We, therefore, aimed to model a sub-stoichiometric, or partial scavenge, of free Hb in vitro, to recapitulate the likely situation in vivo more realistically. As discussed in the introduction, a partial scavenge is more likely to be achievable in a clinical setting because of variable factors in bleed volume and hence Hb concentration, density of the haematoma and modifications to Hb over time making it unable to be bound by Hp (Akeret et al., 2021; Garland et al., 2020; Zhou et al., 2022).

One report suggests Hp can enhance Hb-mediated neuronal death (Chen-Roetling & Regan, 2016), whilst another study showed that the same Hp formulation can prevent Hb toxicity in cultured neurons (Garland et al., 2020). To investigate the possibility of Hp being toxic in itself, we tested Hp alone up to 120 μM and found no impairment of ATP levels, in fact a small increase in ATP was found when 30 μM Hp was applied for 1 week. After applying HL with or without Hp, we found ATP levels were restored when free Hb was reduced to 13.2 ± 0.7 μM or less, regardless of whether 20 or 50 μM HL had been applied initially. In microscopy, complete binding of all free Hb showed a full restoration of neurite integrity, so that even 50 μM of Hb once in complex with Hp was no longer damaging to the cells. In conclusion, free Hb must be reduced to sub-lethal levels of between 13.2–20 μM to prevent neuronal damage as indicated by ATP deficits within our culture system, and this can be achieved using Hp. Furthermore, Hp prevents Hb-induced ATP or microtubule impairment. Our results agree with the recent publication by Garland and colleagues demonstrating that Hp can prevent, rather than enhance, Hb-mediated toxicity (Garland et al., 2020).

Next we measured the function of neurons in the presence of sub-lethal Hb. Previous research suggested that Hb can alter membrane potential (Yip et al., 1996); however, the data were collected at a significantly higher concentration of 0.1 mM Hb, equivalent to 200 μM Hb dimer—a concentration that induced significant loss of ATP in our cultures. We measured intrinsic membrane properties after 1-week exposure to sub-lethal Hb, applying HL at 10 μM, which did not result in an ATP deficit in our system. We found no change to the RMP, input resistance or action potential firing when HL was applied with or without Hp. These data suggest that cultured neurons can maintain their membrane properties in the presence of 10 μM of free Hb. Maintaining a RMP around −70 mV in neurons is an active process, with ATP powering the sodium potassium exchange pump to preserve the correct electrochemical gradients (Zhang et al., 2009). Input resistance is affected by a number of factors including the presence of K^+ leak channels, open synaptic receptor channels and the surface area of cell membrane and affects the excitability of the neuron (Kaczmarek et al., 1980; Sun et al., 2018). Correct RMP and input resistance will affect the level of stimuli required to elicit an action potential and are necessary to keep neurons at an optimal excitability within the neuronal network. These measures, in addition to rheobase and action potential number, were unchanged by 10 μM HL, and therefore, basal membrane properties and neuron excitability are normal in the presence of 10 μM HL, which correlates with a preservation of normal ATP levels under these conditions.

We also studied neurotransmission, especially since prior evidence showed changes in synaptic composition (Garland et al., 2020; Han et al., 2014; Shen et al., 2015) and cognitive impairment after SAH (Al-Khindi et al., 2010; Ellmore et al., 2013; Tariq et al., 2010). We focused on AMPA glutamate receptors, as much of the fast excitatory neurotransmission in the hippocampus is mediated by these tetrameric ionotropic receptors. Rapid depolarisation through AMPARs is typically required to enable action potential firing, following a summated post-synaptic response. We found a reduction in the amplitude of mEPSCs, evoked EPSPs and EPSCs after HL incubation, which provides strong evidence for a reduction in the number of AMPA receptors at the post-synaptic site of recorded neurons. Using Western blotting we also observed a reduction in GluA1 subunit expression in cell cultures, similar to previous research (Han et al., 2014). GluA1 is present in the majority of AMPA receptors in the hippocampus (Lu et al., 2009; Wenthold et al., 1996) and as such, a reduction in expression is likely to cause a reduction in amplitude of excitatory currents.

Research suggests that Hb can also potentiate the excitotoxic effects of other molecules, such as in the presence of excess neurotransmitters (Regan & Scott Panter, 1996). Glutamate-mediated neurotoxicity has been implicated in ischaemic and haemorrhagic stroke (Righy et al., 2015; Schatlo et al., 2010) and lesions in SAH follow the functional neuroanatomy rather than vascular architecture (Schatlo et al., 2010). Iron levels after haemorrhage may play a role in this process by altering glutamate uptake (Yu et al., 2009). Excess glutamate causing excitotoxicity can drive AMPAR internalisation and degradation leading to synaptic depression (Zhang et al., 2009) in a homeostatic downscaling mechanism to preserve neuronal excitability (Hou et al., 2011).

Other contributing factors include alterations to receptor trafficking, which may link to the degree of neurite beading observed in the presence of free Hb. Degradation of microtubules within neurites will disrupt transport pathways within the cell, disturbing intracellular trafficking (Sadleir et al., 2016). This could impair the trafficking of AMPA receptors to synaptic sites, which may have significant implications for synaptic plasticity. Hippocampal LTP requires the

insertion of AMPA receptors into the synaptic membrane (Benke & Traynelis, 2019; Gu et al., 2010; Kessels & Malinow, 2009), and disruptions to trafficking via microtubules in addition to GluA1 protein down-regulation will result in a lower availability of AMPA receptors available to enable long-term potentiation mechanisms. These mechanisms may explain the loss of hippocampal LTP in a rat model of SAH (Tariq et al., 2010), and since LTP is proposed to underpin many learning and memory processes (Bliss & Collingridge, 1993) functional recovery after SAH is also likely impaired by changes to AMPAR availability.

The reduction in AMPAR-mediated currents observed in this study occurred at sub-lethal concentrations of free Hb, which did not impair ATP or cause overt cell death, indicating that neurons in brain regions exposed to low levels of Hb may be surviving but are functionally impaired. Surviving cells exposed to Hb concentrations greater than 10 μM are likely to have even greater impairments in AMPA receptor-driven excitation, as evidence suggests that a reduction in ATP, as seen in our assays at 20 μM HL and above, leads to imbalance of Ca^{2+}, Na^{+}, Ca^{2+} and Cl^{-} ions, inhibiting glutamate reuptake (Nagy & Nardai, 2017). However, we have not measured currents at greater HL concentrations using electrophysiology in this study, as visually guided patch clamp would be subject to selection bias of surviving cells.

We did not find any changes to pre-synaptic measures, including mEPSC frequency, evoked EPSP failure rate or paired-pulse facilitation. We also measured $GABA_A$ mIPSCs and found no change to frequency or amplitude (data are not shown) suggesting sub-lethal Hb selectively impairs the post-synaptic element of AMPAR-mediated excitatory neurotransmission.

Throughout our data on AMPA receptor-mediated transmission, we have seen that partially scavenging free Hb is sufficient to prevent a significant deficit. Hp scavenging of free Hb sequesters it in large stable complexes, preventing release of haem and compartmentalising the pathological species (Buehler et al., 2020; Schaer et al., 2021). In this study it is likely that although we have only sequestered one-third of free Hb, this is sufficient to reduce a 10 μM concentration of Hb dimers to levels below the threshold for excitotoxicity or alteration to synapses; this is promising for the therapeutic potential of Hp.

It is also possible that Hp in itself has beneficial effects beyond binding Hb—for example Hp is well known as an anti-inflammatory protein, expressed in the acute phase response (Moestrup & Møller, 2004). Since Hb breakdown products can activate inflammatory pathways in SAH (Belcher et al., 2014; Fassbender et al., 2001) leading to activation of microglia and their conversion to harmful secretory phenotypes (Kwon et al., 2015; You et al., 2016), Hp may provide neuroprotection beyond scavenging Hb through its anti-inflammatory effects. On its own, Hp did not impair ATP, and in fact, a small increase in ATP levels was observed in neuronal cultures when incubated at 30 μM but no change from vehicle conditions was found at higher concentrations up to 120 μM. Neurite morphology was not altered by Hp, nor were intrinsic membrane properties or AMPA receptor-mediated excitatory currents. At the highest Hp concentration used in our study, Hp levels in culture medium were significantly higher than plasma concentrations (Garland et al., 2020) or those that would be delivered intrathecally for treatment of SAH, which is reassuring.

In conclusion, we isolated Hb neurotoxicity in a neuronal culture model of SAH and observed a dose-dependent impairment of ATP levels and neurite integrity upon long-term exposure to Hb. Clinically relevant, sub-lethal concentrations of Hb caused down-regulation of AMPA receptors at the synapse, which may be because of a combination of altered protein expression levels and trafficking disruption from microtubule disintegration. Partially scavenging of one-third of free Hb using Hp was sufficient to restore AMPA and ATP deficits at 10–20 μM of HL, and Hp itself showed no negative effects even at very high concentrations. This data help explain neurological deficits after SAH and supports the development of Hp as a therapeutic agent to reduce the impact of secondary brain injury after SAH.

AUTHOR CONTRIBUTIONS

HW, KD, DB, IG and MVC designed experiments. H.W. performed experiments, HW, KD and MVC analysed the data. Haptoglobin was obtained and supplied by PG and JM. All authors approved the manuscript.

ACKNOWLEDGMENTS

The authors thank Dr Charlotte Stuart for collection of human RBCs, and Dr Mark Willett and the Imaging and Microscopy Centre at University of Southampton for technical support.

FUNDING INFORMATION

This study was funded by the Gerald Kerkut Charitable Trust and Institute for Life Sciences, University of Southampton.

CONFLICT OF INTEREST STATEMENT

Authors PG and JM are employed by Bio Products Laboratory Ltd and supplied Hp for the study. Design, execution and analysis of experiments was carried out independently of Bio Products Laboratory Ltd. The other authors have no conflicts of interest to declare.

PEER REVIEW

The peer review history for this article is available at https://www.webofscience.com/api/gateway/wos/peer-review/10.1111/jnc.15936.

DATA AVAILABILITY STATEMENT

The data sets used and/or analysed during the current study are available from the corresponding authors on reasonable request. A preprint of this article was posted on BioRxiv on 25th January 2023 https://biorxiv.org/content/10.1101/2023.01.25.525148v1.

ORCID

Hannah Warming https://orcid.org/0000-0001-8740-3571
Katrin Deinhardt https://orcid.org/0000-0002-6473-5298
Patrick Garland https://orcid.org/0000-0002-7679-6426

Diederik Bulters https://orcid.org/0000-0001-9884-9050
Ian Galea https://orcid.org/0000-0002-1268-5102
Mariana Vargas-Caballero https://orcid.org/0000-0003-2326-4001

TWITTER

Hannah Warming WarmingHannah
Katrin Deinhardt KatrinDeinhardt
Mariana Vargas-Caballero synapseMVClab

REFERENCES

Akeret, K., Buzzi, R. M., Schaer, C. A., Thomson, B. R., Vallelian, F., Wang, S., Willms, J., Sebök, M., Held, U., Deuel, J. W., Humar, R., Regli, L., Keller, E., Hugelshofer, M., & Schaer, D. J. (2021). Cerebrospinal fluid hemoglobin drives subarachnoid hemorrhage-related secondary brain injury. *Journal of Cerebral Blood Flow and Metabolism*, *41*, 3000–3015.

Al-Khindi, T., Macdonald, R. L., & Schweizer, T. A. (2010). Cognitive and functional outcome after aneurysmal subarachnoid hemorrhage. *Stroke*, *41*, 519–536.

Bai, Q., Liu, J., & Wang, G. (2020). Ferroptosis, a regulated neuronal cell death type after intracerebral hemorrhage. *Frontiers in Cellular Neuroscience*, *14*, 374.

Belcher, J. D., Chen, C., Nguyen, J., Milbauer, L., Abdulla, F., Alayash, A. I., Smith, A., Nath, K. A., Hebbel, R. P., & Vercellotti, G. M. (2014). Heme triggers TLR4 signaling leading to endothelial cell activation and vaso-occlusion in murine sickle cell disease. *Blood*, *123*, 377–390.

Benesch, R. E., Benesch, R., & Yung, S. (1973). Equations for the spectrophotometric analysis of hemoglobin mixtures. *Analytical Biochemistry*, *55*, 245–248.

Benke, T., & Traynelis, S. F. (2019). AMPA-type glutamate receptor conductance changes and plasticity: Still a lot of noise. *Neurochemical Research*, *44*, 539–548.

Bliss, T. V. P., & Collingridge, G. L. (1993). A synaptic model of memory: long-term potentiation in the hippocampus. *Nature*, *361*, 31–39.

Budohoski, K. P., Guilfoyle, M., Helmy, A., Huuskonen, T., Czosnyka, M., Kirollos, R., Menon, D. K., Pickard, J. D., & Kirkpatrick, P. J. (2014). The pathophysiology and treatment of delayed cerebral ischaemia following subarachnoid haemorrhage. *Journal of Neurology, Neurosurgery, and Psychiatry*, *85*, 1343–1353.

Buehler, P. W., Humar, R., & Schaer, D. J. (2020). Haptoglobin Therapeutics and Compartmentalization of Cell-Free Hemoglobin Toxicity. *Trends in Molecular Medicine*, *26*, 683–697.

Chen-Roetling, J., & Regan, R. F. (2016). Haptoglobin increases the vulnerability of CD163-expressing neurons to hemoglobin. *Journal of Neurochemistry*, *139*, 586–595.

Diringer, M. N. (2009). Management of aneurysmal subarachnoid hemorrhage. *Critical Care Medicine*, *37*, 432–440.

Diringer, M. N., Bleck, T. P., Hemphill, J. C., Menon, D., Shutter, L., Vespa, P., Bruder, N., Connolly, E. S., Citerio, G., Gress, D., Hänggi, D., Hoh, B. L., Lanzino, G., Le Roux, P., Rabinstein, A., Schmutzhard, E., Stocchetti, N., Suarez, J. I., Treggiari, M., … Zipfel, G. (2011). Critical care management of patients following aneurysmal subarachnoid hemorrhage: recommendations from the Neurocritical Care Society's Multidisciplinary Consensus Conference. *Neurocritical Care*, *15*, 211–240.

Ellmore, T. M., Rohlffs, F., & Khursheed, F. (2013). FMRI of working memory impairment after recovery from subarachnoid hemorrhage. *Frontiers in Neurology*, *4*, 179.

English, S. W. (2020). Long-term outcome and economic burden of aneurysmal subarachnoid hemorrhage: Are we only seeing the tip of the iceberg? *Neurointensive Care*, *33*, 37–38.

Fassbender, K., Hodapp, B., Rossol, S., Bertsch, T., Schmeck, J., Schütt, S., Fritzinger, M., Horn, P., Vajkoczy, P., Kreisel, S., Brunner, J., Schmiedek, P., & Hennerici, M. (2001). Inflammatory cytokines in subarachnoid haemorrhage: Association with abnormal blood flow velocities in basal cerebral arteries. *Journal of Neurology, Neurosurgery, and Psychiatry*, *70*, 534–537.

Gaastra, B., Glazier, J., Bulters, D., & Galea, I. (2017). Haptoglobin genotype and outcome after subarachnoid haemorrhage: New insights from a meta-analysis. *Oxidative Medicine and Cellular Longevity*, *2017*, 1–9.

Galea, I. (2021). The blood–brain barrier in systemic infection and inflammation. *Cellular & Molecular Immunology*, *18*, 2489–2501.

Galea, I., Durnford, A., Glazier, J., Mitchell, S., Kohli, S., Foulkes, L., Norman, J., Darekar, A., Love, S., Bulters, D. O., Nicoll, J. A. R., & Boche, D. (2022). Iron deposition in the brain after aneurysmal subarachnoid hemorrhage. *Stroke*, *53*, 1633–1642.

Galea, J., Cruickshank, G., Teeling, J. L., Boche, D., Garland, P., Perry, V. H., & Galea, I. (2012). The intrathecal CD163-haptoglobin-hemoglobin scavenging system in subarachnoid hemorrhage. *Journal of Neurochemistry*, *121*, 785–792.

Gando, S., & Tedo, I. (1994). The effects of massive transfusion and haptoglobin therapy on hemolysis in trauma patients. *Surgery Today*, *24*, 785–790.

Garland, P., Broom, L. J., Quraishe, S., Dalton, P. D., Skipp, P., Newman, T. A., & Perry, V. H. (2012). Soluble axoplasm enriched from injured CNS axons reveals the early modulation of the actin cytoskeleton. *PLoS One*, *7*, e47552.

Garland, P., Morton, M., Zolnourian, A., Durnford, A., Gaastra, B., Toombs, J., Heslegrave, A. J., More, J., Zetterberg, H., Bulters, D. O., & Galea, I. (2021). Neurofilament light predicts neurological outcome after subarachnoid haemorrhage. *Brain*, *144*, 761–768.

Garland, P., Morton, M. J., Haskins, W., Zolnourian, A., Durnford, A., Gaastra, B., Toombs, J., Heslegrave, A. J., More, J., Okemefuna, A. I., Teeling, J. L., Graversen, J. H., Zetterberg, H., Moestrup, S. K., Bulters, D. O., & Galea, I. (2020). Haemoglobin causes neuronal damage in vivo which is preventable by haptoglobin. *Brain Communications*, *2*, fcz053.

Garton, T. P., He, Y., Garton, H. J. L., Keep, R. F., Xi, G., & Strahle, J. M. (2016). Hemoglobin-induced neuronal degeneration in the hippocampus after neonatal intraventricular hemorrhage. *Brain Research*, *1635*, 86–94.

Gu, J., Lee, C. W., Fan, Y., Komlos, D., Tang, X., Sun, C., Yu, K., Hartzell, H. C., Chen, G., Bamburg, J. R., & Zheng, J. Q. (2010). ADF/cofilin-mediated actin dynamics regulate AMPA receptor trafficking during synaptic plasticity. *Nature Neuroscience*, *13*, 1208–1215.

Hackett, M. L., & Anderson, C. S. (2000). Health outcomes 1 year after subarachnoid hemorrhage an international population-based study. *Neurology*, *55*, 658–662.

Han, S. M., Wan, H., Kudo, G., Foltz, W. D., Vines, D. C., Green, D. E., Zoerle, T., Tariq, A., Brathwaite, S., D'Abbondanza, J., Ai, J., & Macdonald, R. L. (2014). Molecular alterations in the hippocampus after experimental subarachnoid hemorrhage. *Journal of Cerebral Blood Flow and Metabolism*, *34*, 108–117.

Hilgenberg, L. G. W. W., & Smith, M. A. (2007). Preparation of dissociated mouse cortical neuron cultures. *Journal of Visualized Experiments*, *10*, e562. https://doi.org/10.3791/562

Hou, Q., Gilbert, J., & Man, H. Y. (2011). Homeostatic regulation of AMPA receptor trafficking and degradation by light-controlled single-synaptic activation. *Neuron*, *72*, 806–818.

Hugelshofer, M., Buzzi, R. M., Schaer, C. A., Richter, H., Akeret, K., Anagnostakou, V., Mahmoudi, L., Vaccani, R., Vallelian, F., Deuel, J. W., Kronen, P. W., Kulcsar, Z., Regli, L., Baek, J. H., Pires, I. S., Palmer, A. F., Dennler, M., Humar, R., Buehler, P. W., … Schaer, D. J. (2019). Haptoglobin administration into the subarachnoid space prevents hemoglobin-induced cerebral vasospasm. *The Journal of Clinical Investigation*, *129*, 5219.

Hugelshofer, M., Sikorski, C. M., Seule, M., Deuel, J., Muroi, C. I., Seboek, M., Akeret, K., Buzzi, R., Regli, L., Schaer, D. J., & Keller, E. (2018).

Cell-free oxyhemoglobin in cerebrospinal fluid after aneurysmal subarachnoid hemorrhage: biomarker and potential therapeutic target. *World Neurosurgery*, *120*, e660–e666.

Hui, C. W., Zhang, Y., & Herrup, K. (2016). Non-neuronal cells are required to mediate the effects of neuroinflammation: Results from a neuron-enriched culture system. *PLoS One*, *11*, e0147134.

Janick, P. A., Hackney, D. B., Grossman, R. I., & Asakura, T. (1991). MR imaging of various oxidation states of intracellular and extracellular hemoglobin. *American Journal of Neuroradiology*, *12*, 891–897.

Jeffcote, T., & Ho, K. M. (2010). Associations between cerebrospinal fluid protein concentrations, serum albumin concentrations and intracranial pressure in neurotrauma and intracranial haemorrhage. *Anaesth. Intensive Care*, *38*, 274–279.

Jellinger, K. A. (1999). The role of iron in neurodegeneration. Prospects for pharmacotherapy of Parkinson's disease. *Drugs and Aging*, *14*, 115–140.

Joerk, A., Seidel, R. A., Walter, S. G., Wiegand, A., Kahnes, M., Klopfleisch, M., Kirmse, K., Pohnert, G., Westerhausen, M., Witte, O. W., & Holthoff, K. (2014). Impact of heme and heme degradation products on vascular diameter in mouse visual cortex. *Journal of the American Heart Association*, *3*, e001220.

Jungner, Å., Vallius Kvist, S., Romantsik, O., Bruschettini, M., Ekström, C., Bendix, I., Herz, J., Felderhoff-Mueser, U., Bibic, A., In'T Zandt, R., Gram, M., & Ley, D. (2020). White matter brain development after exposure to circulating cell-free hemoglobin and hyperoxia in a rat pup model. *Developmental Neuroscience*, *41*, 234–246.

Kaczmarek, L. K., Jennings, K. R., Strumwasser, F., Nairn, A. C., Walter, U., Wilson, F. D., & Greengard, P. (1980). Microinjection of catalytic subunit of cyclic AMP-dependent protein kinase enhances calcium action potentials of bag cell neurons in cell culture. *Proceedings of the National Academy of Sciences*, *77*, 7487–7491.

Kazmi, N., Koda, Y., Ndiaye, N. C., Visvikis-Siest, S., Morton, M. J., Gaunt, T. R., & Galea, I. (2019). Genetic determinants of circulating haptoglobin concentration. *Clinica Chimica Acta*, *494*, 138–142.

Kessels, H. W., & Malinow, R. (2009). Synaptic AMPA receptor plasticity and behavior. *Neuron*, *61*, 340–350.

Kwon, M. S., Woo, S. K., Kurland, D. B., Yoon, S. H., Palmer, A. F., Banerjee, U., Iqbal, S., Ivanova, S., Gerzanich, V., & Simard, J. M. (2015). Methemoglobin is an endogenous Toll-like receptor 4 ligand—relevance to subarachnoid hemorrhage. *International Journal of Molecular Sciences*, *16*, 5028–5046.

Kwon, S. K., & Kim, M. W. (2014). Pseudo-Froin's syndrome, xanthochromia with high protein level of cerebrospinal fluid. *Korean Journal of Anesthesiology*, *67*, S58.

Li, Q., Han, X., Lan, X., Gao, Y., Wan, J., Durham, F., Cheng, T., Yang, J., Wang, Z., Jiang, C., Ying, M., Koehler, R. C., Stockwell, B. R., & Wang, J. (2017). Inhibition of neuronal ferroptosis protects hemorrhagic brain. *JCI Insight*, *2*, e90777.

Lu, W., Shi, Y., Jackson, A. C., Bjorgan, K., During, M. J., Sprengel, R., Seeburg, P. H., & Nicoll, R. A. (2009). Subunit composition of synaptic AMPA receptors revealed by a single-cell genetic approach. *Neuron*, *62*, 254–268.

Luoma, A., & Reddy, U. (2013). Acute management of aneurysmal subarachnoid haemorrhage. *Continuing Education in Anaesthesia, Critical Care and Pain*, *13*, 52–58.

McCudden, C. R., Brooks, J., Figurado, P., & Bourque, P. R. (2017). Cerebrospinal fluid total protein reference intervals derived from 20 years of patient data. *Clinical Chemistry*, *63*, 1856–1865.

Moestrup, S., & Møller, H. (2004). CD163: a regulated hemoglobin scavenger receptor with a role in the anti-inflammatory response. *Annals of Medicine*, *36*, 347–354.

Nadkarni, N. A., Maas, M. B., Batra, A., Kim, M., Manno, E. M., Sorond, F. A., Prabhakaran, S., Naidech, A. M., & Liotta, E. M. (2020). Elevated cerebrospinal fluid protein is associated with unfavorable functional outcome in spontaneous subarachnoid hemorrhage. *Journal of Stroke and Cerebrovascular Diseases*, *29*, 104605.

Nagy, Z., & Nardai, S. (2017). Cerebral ischemia/repefusion injury: From bench space to bedside. *Brain Research Bulletin*, *134*, 30–37.

Neifert, S. N., Chapman, E. K., Martini, M. L., Shuman, W. H., Schupper, A. J., Oermann, E. K., Mocco, J., & Macdonald, R. L. (2021). Aneurysmal subarachnoid hemorrhage: the Last decade. *Translational Stroke Research*, *12*, 428–446.

Patel, B. N., Dunn, R. J., Jeong, S. Y., Zhu, Q., Julien, J. P., & David, S. (2002). Ceruloplasmin regulates iron levels in the CNS and prevents free radical injury. *The Journal of Neuroscience*, *22*, 6578–6586.

Penke, L., Valdés Hernandéz, M. C., Maniega, S. M., Gow, A. J., Murray, C., Starr, J. M., Bastin, M. E., Deary, I. J., & Wardlaw, J. M. (2012). Brain iron deposits are associated with general cognitive ability and cognitive aging. *Neurobiology of Aging*, *33*, 510–517.e2.

Petridis, A. K., Kamp, M. A., Cornelius, J. F., Beez, T., Beseoglu, K., Turowski, B., & Steiger, H. J. (2017). Aneurysmal subarachnoid hemorrhage-diagnosis and treatment. *Deutsches Ärzteblatt International*, *114*, 226–235.

Pluta, R. M., Afshar, J. K. B., Boock, R., & Oldfield, E. H. (1998). Temporal changes in perivascular concentrations of oxyhemoglobin, deoxyhemoglobin, and methemoglobin after subarachnoid hemorrhage. *Journal of Neurochemistry*, *88*, 557–561.

Regan, R. F., & Guo, Y. (1998). Toxic effect of hemoglobin on spinal cord neurons in culture. *Journal of Neurotrauma*, *15*, 645–653.

Regan, R. F., & Panter, S. S. (1993). Neurotoxicity of hemoglobin in cortical cell culture. *Neuroscience Letters*, *153*, 219–222.

Regan, R. F., & Scott Panter, S. (1996). Hemoglobin potentiates excitotoxic injury in cortical cell culture. *Journal of Neurotrauma*, *13*, 223–231.

Righy, C., Bozza, T. M., Oliveira, M. F., & Bozza, F. A. (2015). Molecular, cellular and clinical aspects of intracerebral hemorrhage: are the enemies within? *Current Neuropharmacology*, *14*, 392–402.

Sadleir, K. R., Kandalepas, P. C., Buggia-Prévot, V., Nicholson, D. A., Thinakaran, G., & Vassar, R. (2016). Presynaptic dystrophic neurites surrounding amyloid plaques are sites of microtubule disruption, BACE1 elevation, and increased Aβ generation in Alzheimer's disease. *Acta Neuropathologica*, *132*, 235–256.

Sadrzadeh, S. M. H., & Bozorgmehr, J. (2004). Haptoglobin phenotypes in health and disorders. *American Journal of Clinical Pathology*, *121*, S97–S104.

Sasaki, T., Hoffmann, U., Kobayashi, M., Sheng, H., Ennaceur, A., Lombard, F. W., & Warner, D. S. (2016). Long-term cognitive deficits after subarachnoid hemorrhage in rats. *Neurocritical Care*, *25*, 293–305.

Schaer, C. A., Jeger, V., Gentinetta, T., Spahn, D. R., Vallelian, F., Rudiger, A., & Schaer, D. J. (2021). Haptoglobin treatment prevents cell-free hemoglobin exacerbated mortality in experimental rat sepsis. *Intensive Care Medicine Experimental*, *9*, 1–4.

Schaer, D. J., Buehler, P. W., Alayash, A. I., Belcher, J. D., & Vercellotti, G. M. (2013). Hemolysis and free hemoglobin revisited: exploring hemoglobin and hemin scavengers as a novel class of therapeutic proteins. *Blood*, *121*, 1276–1284.

Schatlo, B., Dreier, J. P., Gläsker, S., Fathi, A. R., Moncrief, T., Oldfield, E. H., Vortmeyer, A. O., & Pluta, R. M. (2010). Report of selective cortical infarcts in the primate clot model of vasospasm after subarachnoid hemorrhage. *Neurosurgery*, *67*, 721–728.

Schilling, T., & Eder, C. (2015). Microglial K+ channel expression in young adult and aged mice. *Glia*, *63*, 664–672.

Schindelin, J., Arganda-Carreras, I., Frise, E., Kaynig, V., Longair, M., Pietzsch, T., Preibisch, S., Rueden, C., Saalfeld, S., Schmid, B., Tinevez, J. Y., White, D. J., Hartenstein, V., Eliceiri, K., Tomancak, P., & Cardona, A. (2012). Fiji: an open-source platform for biological-image analysis. *Nature Methods*, *97*(9), 676–682.

Shen, H., Chen, Z., Wang, Y., Gao, A., Li, H., Cui, Y., Zhang, L., Xu, X., Wang, Z., & Chen, G. (2015). Role of neurexin-1β and neuroligin-1 in cognitive dysfunction after subarachnoid hemorrhage in rats. *Stroke*, *46*, 2607–2615.

Siddiqui, F. M., Bekker, S. V., & Qureshi, A. I. (2011). Neuroimaging of hemorrhage and vascular defects. *Neurotherapeutics*, *8*, 28.

Sun, Z., Williams, D. J., Xu, B., & Gogos, J. A. (2018). Altered function and maturation of primary cortical neurons from a 22q11.2 deletion mouse model of schizophrenia. *Transl. Psychiatry*, *8*, 1–14.

Tariq, A., Ai, J., Chen, G., Sabri, M., Jeon, H., Shang, X., & Macdonald, R. L. (2010). Loss of long-term potentiation in the hippocampus after experimental subarachnoid hemorrhage in rats. *Neuroscience*, *165*, 418–426.

Thomsen, J. H., Etzerodt, A., Svendsen, P., & Moestrup, S. K. (2013). The haptoglobin-CD163-heme oxygenase-1 pathway for hemoglobin scavenging. *Oxidative Medicine and Cellular Longevity*, *2013*, 523652.

Tidswell, P., Dias, P. S., Sagar, H. J., Mayes, A. R., & Battersby, R. D. E. (1995). Cognitive outcome after aneurysm rupture: Relationship to aneurysm site and perioperative complications. *Neurology*, *45*, 876–882.

Van Gijn, J., & Rinkel, G. J. E. (2001). Subarachnoid haemorrhage: Diagnosis, causes and management. *Brain*, *124*, 249–278.

Wang, X., Mori, T., Sumii, T., & Lo, E. H. (2002). Hemoglobin-induced cytotoxicity in rat cerebral cortical neurons: Caspase activation and oxidative stress. *Stroke*, *33*, 1882–1888.

Wenthold, R. J., Petralia, R. S., Blahos, J., & Niedzielski, A. S. (1996). Evidence for multiple AMPA receptor complexes in hippocampal CA1/CA2 neurons. *The Journal of Neuroscience*, *16*, 1982–1989.

Winchester, G., Liu, S., Steele, O.G., Aziz, W., & Penn, A. (2020). Eventer. Software for the detection of spontaneous synaptic events measured by electrophysiology or imaging, https://doi.org/10.5281/ZENODO.3991677.

Yeh, L. H., & Alayash, A. I. (2003). Redox side reactions of haemoglobin and cell signalling mechanisms. *Journal of Internal Medicine*, *253*, 518–526.

Yip, S., Ip, J. K. H., & Sastry, B. R. (1996). Electrophysiological actions of hemoglobin on rat hippocampal CA1 pyramidal neurons. *Brain Research*, *713*, 134–142.

You, W., Wang, Z., Li, H., Shen, H., Xu, X., Jia, G., & Chen, G. (2016). Inhibition of mammalian target of rapamycin attenuates early brain injury through modulating microglial polarization after experimental subarachnoid hemorrhage in rats. *Journal of the Neurological Sciences*, *367*, 224–231.

Yu, J., Guo, Y., Sun, M., Li, B., Zhang, Y., & Li, C. (2009). Iron is a potential key mediator of glutamate excitotoxicity in spinal cord motor neurons. *Brain Research*, *1257*, 102–107.

Zhang, D., Hou, Q., Wang, M., Lin, A., Jarzylo, L., Navis, A., Raissi, A., Liu, F., & Man, H. Y. (2009). Na,K-ATPase activity regulates AMPA receptor turnover through proteasome-mediated proteolysis. *The Journal of Neuroscience*, *29*, 4498–4511.

Zhou, J., Guo, P., Guo, Z., Sun, X., Chen, Y., & Feng, H. (2022). Fluid metabolic pathways after subarachnoid hemorrhage. *Journal of Neurochemistry*, *160*, 13–33.

Zille, M., Karuppagounder, S. S., Chen, Y., Gough, P. J., Bertin, J., Finger, J., Milner, T. A., Jonas, E. A., & Ratan, R. R. (2017). Neuronal death after hemorrhagic stroke in vitro and in vivo shares features of ferroptosis and necroptosis. *Stroke*, *48*, 1033–1043.

How to cite this article: Warming, H., Deinhardt, K., Garland, P., More, J., Bulters, D., Galea, I., & Vargas-Caballero, M. (2023). Functional effects of haemoglobin can be rescued by haptoglobin in an in vitro model of subarachnoid haemorrhage. *Journal of Neurochemistry*, *167*, 90–103. https://doi.org/10.1111/jnc.15936